Soil Dynamics and Earthquake Engineering 44 (2013) 14–26

Contents lists available at SciVerse ScienceDirect

Soil Dynamics and Earthquake Engineering

journal homepage: www.elsevier.com/locate/soildyn

# Three-dimensional dynamic transient response of a poro-elastic unsaturated seabed and a rubble mound breakwater due to seismic loading

J.H. Ye [b], D.-S. Jeng [a,b,*]

[a] Center for Marine Geotechnical Engineering, Shanghai Jiao Tong University, Shanghai 200240, China
[b] Division of Civil Engineering, University of Dundee, DD1 4HN, UK

ARTICLE INFO

*Article history:*
Received 5 January 2012
Received in revised form
2 August 2012
Accepted 19 August 2012

ABSTRACT

Marine infrastructures are generally vulnerable to strong seismic waves propagating through their seabed foundation. However, only limited attentions have been given to the dynamic seabed response around marine structures under strong seismic loading in the past, although numerous cases of failure of marine infrastructures during strong earthquake events have been reported in the literature. In this study, employing the dynamic Biot's equation as the governing equation, in which the accelerations of both soil and pore water are considered, a three-dimensional (3D) FEM soil model for consolidation and dynamic analysis is developed. With the proposed model, the dynamic response of a rubble mound breakwater and its porous seabed foundation under the seismic wave recorded in the Japan 311 off the pacific coast of Tohoku earthquake ($M_L$ magnitude = 9.0) is investigated. Numerical results indicate that the rubble mound breakwater vibrates strongly in the earthquake process. The porous seabed foundation amplifies the seismic wave significantly from the bottom to the surface.



## 1. Introduction

In the last two decades, constructions of marine infrastructures such as breakwaters, oil platforms and wind turbines have been dramatically growing up due to economic activities. The stability of these marine structures under the environmental loading is the main concern for the coastal and geotechnical engineers involved in the design processes. As a kind of marine structures, rubble mound breakwaters have been widely adopted for the protection of coastal zones worldwide, especially in Japan and Spain. In general, two types of environmental loading in offshore environment have been considered in the design of marine structures. One is hydrodynamic loading (including waves and currents) and the other is the earthquake induced loading. In this study, the second-type of environmental loading–seismic loading will be studied.

In engineering practice, the seismic coefficient method based on the static analysis is widely adopted to simply consider the seismic response of breakwater against the earthquake damage. The seismic loading is not a conventional loading for breakwaters, because a strong earthquake may not occur in the zones near marine infrastructures. However, once an earthquake occurs nearby, the damage to these marine structures would be devastating. For example, the failure of marine structure in Los Angeles (USA) in 1994, Kobe (Japan) in 1995, Kocaeli (Turkey) in 1999; Athens (Greece) in 1999 and Sumatra (Indonesia) in 2003. Numerous cases of the earthquake induced failure of marine structures have been reported in the literature [1–4]. Therefore, besides the wave loading, the seismic loading should be considered for some important structures built in active seismic zone, for example, the east coast of Japan. More sophisticated seismic response analysis is needed, rather than adopting the quasi-static design method.

Dynamic response of breakwaters under wave loading has been extensively studied since the 1980s [5]. To date, the experimental and numerical investigation on the seismic response of a rubble mound breakwater under earthquake loading have been limited. Among these, Yuksel et al. [4] analyzed the seismic wave induced deformation of breakwater at the Eregli Fishery port during 1999 Koceali Turkey earthquake based on the material obtained from the field sites. A series of shaking table tests were carried out to investigate the seismic response and stability of a rubble mound breakwater, together with numerical study [6,7]. The dynamic water pressure acting on the outer surface of the rubble mound breakwater was taken into consideration based on the Westerggard's equation [8]. In their experiments, they found the response acceleration related to the depth of sandy bed is ignorable; and the sandy bed plays a dominant role in the prediction of the breakwater failure. Similar shaking table tests were also conducted by [9]. Based on the previous experimental data [6,7], Memos et al. [10] further numerically investigated the seismic response of rubble mound breakwater

* Corresponding author at: Division of Civil Engineering, University of Dundee, DD1 4HN, UK. Tel.: +44 1382386141; fax: +44 1382384816.
*E-mail addresses:* d.jeng@dundee.ac.uk, jengd2@asme.org (D.-S. Jeng).

0267-7261/$ - see front matter © 2012 Elsevier Ltd. All rights reserved.
http://dx.doi.org/10.1016/j.soildyn.2012.08.011

using a coupled model, in which the boundary element method is used to solve the fluid domain. The coupling process is implemented through the iteration and the continuity of displacement at the interface between the rubble mound breakwater and water. However, the governing equations for sandy bed and pore fluid were not presented, and the input motion was only harmonic shaking, not a real seismic wave.

Recently, Jafarian et al. [11] adopted the commercial software FLAC to estimate the permanent displacement, in which the Mohr–Coulomb constitutive model and the pore pressure built-up model [12] were used. Due to the fact that the Mohr–Coulomb model used is a simplified model, this method is only applicable to limited cases. Later, Cihan and Yuksel [13] further investigated the deformation of a rubble mound breakwater under horizontal harmonic vibration. In their experiments, it was found that the rubble mound breakwater would collapse under strong vibrations. In their numerical study, the commercial software PLAXIS was adopted. The horizontal harmonic vibrations were applied to the base of the breakwater. However, neither pore water in a rubble mound breakwater nor dynamic pressure acting on the lateral sides of the breakwater induced by the vibration of the breakwater were considered. All the aforementioned numerical models for the seismic analysis of rubble mound breakwaters have been limited to 2D. To the authors' best knowledge, the investigation regarding the seismic response of a rubble mound breakwater in 3D has not been available in the literature.

Generally speaking, the seabed response under dynamic loadings (e.g., wave, currents, earthquakes, etc.) consists of two components, i.e., transient and progressive. For the progressive mechanism, the mean of pore pressures will be built up during the loading, which has been studied by most earthquake engineers. For the transient mechanism, it is an oscillatory fluctuation of pore pressure around the mean (i.e., the build-up pore pressures). In engineering practice, the probability of residual (i.e., pore pressure build-up) liquefaction of a seabed foundation needs to be evaluated through some measurements before breakwater is constructed, such as the SPT, relative density $D_r$ and speed of $P$ and $S$ wave, etc. If the seabed foundation of a site is evaluated that it is quite possible to liquefy, it is not advisable to have construction of marine structures. The seabed with high relative density and SPT is generally chosen as the foundation of marine structures, because the rearrangement of soil particles and compaction of in situ soil are unlikely to occur under dynamic loading. However, due to the impulsive loading of earthquakes, the transient liquefaction may still occur, as the upward seepage force becomes greater than the self-weight of soil. Since the build-up of pore pressure will not considered in the transient mode, a poro-elastic theory can be used for the simulation of dynamic response. In this study, we will focus on the second mechanism.

In this study, based on Biot's dynamic poro-elastic theory ("$u-p$" approximation [14]), in which the accelerations of soil particles are considered, a 3D FEM program is further developed. This model is developed on the basis of the 2D FEM program DIANA SWANDYNE-II [15,16]. By adopting the developed 3D numerical model, the seismic response of a rubble mould breakwater resting on a 3D poro-elastic seabed under a strong earthquake loading is investigated numerically.

## 2. Boundary value problem

### 2.1. Governing equation and model verification

It has been well known that seabed is a porous medium consisting of soil particles, pore water and trapped air. Biot's poro-elastic theory has been widely adopted to describe the mechanical behavior of a porous medium. In this study, the seabed is treated as a poro-elastic, isotropic and homogeneous porous medium. The computational domain adopted is shown in Fig. 1. Biot's dynamic poro-elastic theory [17], the "$u-p$" approximation [14], is used as the governing equation for porous seabed and the rubble mound breakwater. The relative displacements of pore fluid to the soil particles are ignored, however, the accelerations of soil particles are included.

Based on conservation of mass and force balances, the governing equations can be expressed as

$$\frac{\partial \sigma'_x}{\partial x}+\frac{\partial \tau_{xy}}{\partial y}+\frac{\partial \tau_{xz}}{\partial z}=-\frac{\partial p_s}{\partial x}+\rho\frac{\partial^2 u_s}{\partial t^2}, \tag{1}$$

$$\frac{\partial \tau_{xy}}{\partial x}+\frac{\partial \sigma'_y}{\partial y}+\frac{\partial \tau_{yz}}{\partial z}=-\frac{\partial p_s}{\partial y}+\rho\frac{\partial^2 v_s}{\partial t^2}, \tag{2}$$

$$\frac{\partial \tau_{xz}}{\partial x}+\frac{\partial \tau_{yz}}{\partial y}+\frac{\partial \sigma'_z}{\partial z}+\rho g=-\frac{\partial p_s}{\partial z}+\rho\frac{\partial^2 w_s}{\partial t^2}, \tag{3}$$

$$k\nabla^2 p_s-\gamma_w n\beta\frac{\partial p_s}{\partial t}+k\rho_f\frac{\partial^2 \epsilon}{\partial t^2}=\gamma_w\frac{\partial \epsilon}{\partial t}, \tag{4}$$

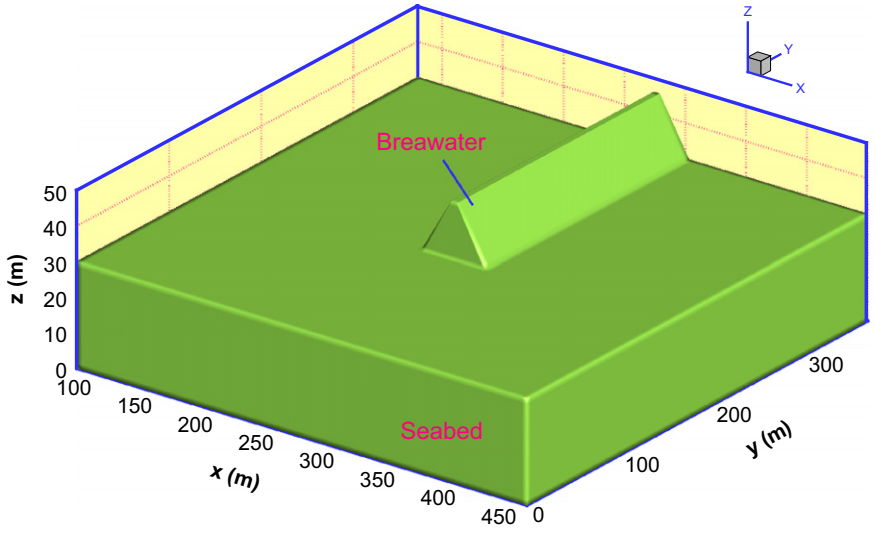


**Fig. 1.** The computational domain of the 3D seabed and breakwater.

where $(u_s, v_s, w_s)$ represents the soil displacements in the $x$-, $y$-, $z$-directions, respectively; $n$ is soil porosity; $\sigma'_x$, $\sigma'_y$ and $\sigma'_z$ are effective normal stresses in the horizontal and vertical directions, respectively; $\tau_{xy}$, $\tau_{xz}$ and $\tau_{yz}$ are shear stresses; $p_s$ denotes the pore pressure in seabed; $\rho = \rho_f n + \rho_s(1-n)$ is the average density of porous seabed; $\rho_f$ is the fluid density; $\rho_s$ is solid density; $k$ is the Darcy's permeability (an isotropic seabed is considered in this study); $g$ is the gravitational acceleration and $\epsilon$ is the volumetric strain. In Eq. (4), the compressibility of pore fluid ($\beta$) and the volume strain ($\epsilon$) are defined as

$$\beta = \left(\frac{1}{K_f} + \frac{1-S_r}{p_{w0}}\right), \quad \text{and} \quad \epsilon = \frac{\partial u_s}{\partial x} + \frac{\partial v_s}{\partial y} + \frac{\partial w_s}{\partial z}, \tag{5}$$

where $S_r$ is the degree of saturation of seabed, $p_{w0}$ is the absolute static pressure and $K_f$ is the bulk modulus of pore water.

In this study, the poro-elastic constitute model is used to describe the soil behavior. Then, the effective normal stresses and shear stresses can be expressed in term of soil displacements,

$$\begin{aligned}
&\sigma'_x = 2G\left[\frac{\partial u}{\partial x} + \frac{\mu}{1-2\mu}\epsilon\right], \quad \sigma'_y = 2G\left[\frac{\partial v}{\partial y} + \frac{\mu}{1-2\mu}\epsilon\right],\\
&\sigma'_z = 2G\left[\frac{\partial w}{\partial z} + \frac{\mu}{1-2\mu}\epsilon\right], \quad \tau_{xz} = G\left[\frac{\partial u}{\partial z} + \frac{\partial w}{\partial x}\right] = \tau_{zx},\\
&\tau_{yz} = G\left[\frac{\partial v}{\partial z} + \frac{\partial w}{\partial y}\right] = \tau_{zy}, \quad \tau_{xy} = G\left[\frac{\partial u}{\partial y} + \frac{\partial v}{\partial x}\right] = \tau_{yx},
\end{aligned} \tag{6}$$

where the shear modulus $G$ is related to Young's modulus $E$ by the Poisson's ratio $\mu$ in the form of $E/2(1+\mu)$.

The above governing equations are solved by adopting a 3D FEM program, which was developed based on the 2D FEM program DIANA SWANDYNE-II [15,16]. This 3D FEM program is actually an extension of the 2D FEM program DIANA SWANDYNE-II. DIANA SWANDYNE-II has been widely verified by a range of laboratory tests, e.g., VELACS project [16]. The capability of the developed 3D FEM program to model the seismic response of soil also has been documented by [18] adopting the model 12 of VELACS project. Herein, the centrifuge test conducted by Elgamal et al. [19] is used to further validate this 3D FEM program through the acceleration response.

Elgamal et al. [19] conducted a series of centrifuge tests to investigate the dynamics of an embankment foundation under seismic wave loading. Here, the tests in which the embankment foundation consisting of Nevada loose sand ($D_r$=40%) is adopted for the verification of the proposed numerical model. The experimental setup is shown in Fig. 2. A clayed sand (mixture of Kaolin clay and Nevada sand (1:4 weight ratio) embankment was built on the Nevada loose sand ($D_r$=40%)). The Nevada loose sand foundation was saturated with a prototype permeability coefficient $k = 5.5 \times 10^{-4}$ m/s. The centrifuge test was performed at the acceleration of 75$g$. One-dimensional horizontal harmonic shaking wave was applied along the model long axis. The maximum acceleration is 0.18$g$; and the frequency is 1.6 Hz (see Fig. 3 (b)). Totally, there are 10 cycles in the input harmonic horizontal shaking.

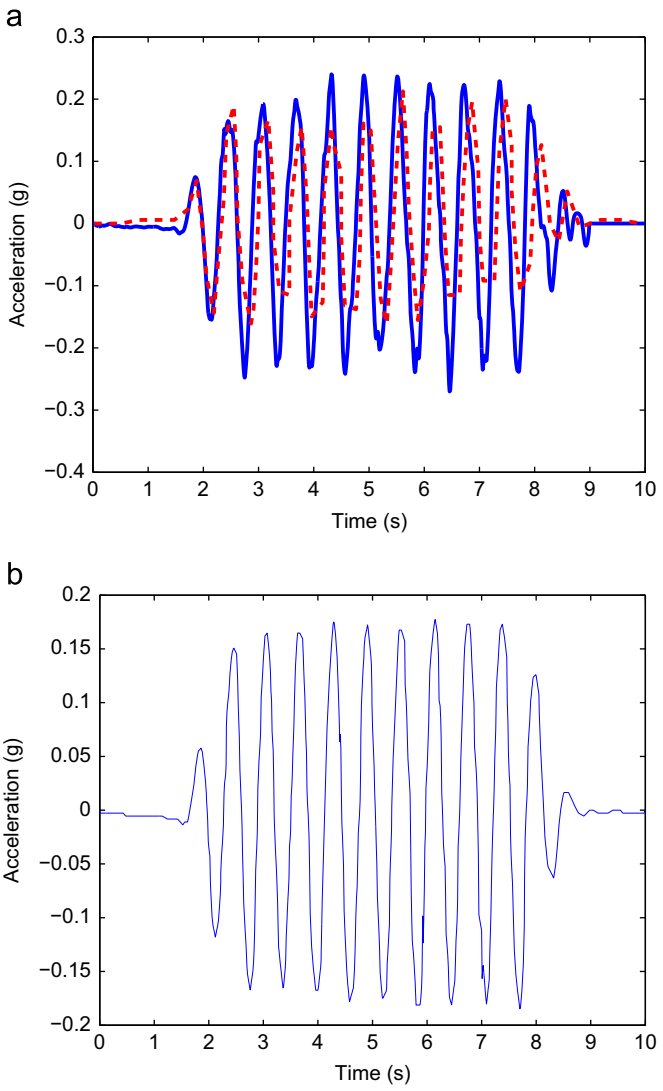


**Fig. 3.** Input harmonic horizontal excitation and comparison between the numerical results and experimental acceleration data. (a) Comparison (solid lines=numerical results, dashed lines=experimental data). (b) Input harmonic horizontal excitation.

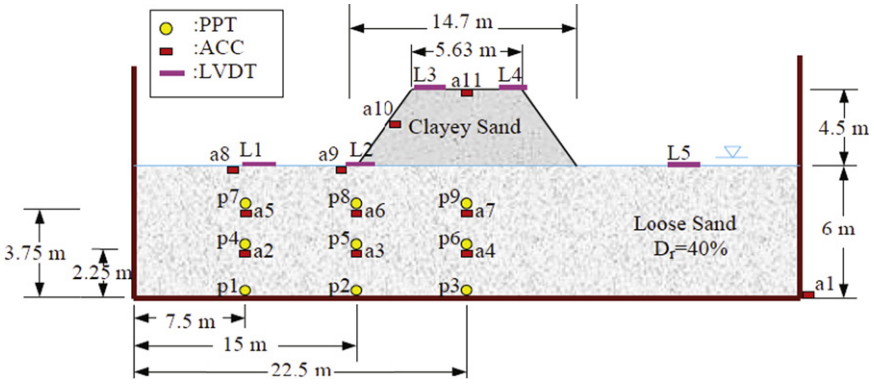


**Fig. 2.** The experimental set up of the centrifuge test conducted by Elgamal et al. [19]. Note: all dimensions have been scaled by 75$g$.

According to the parameters reported in [16], the parameters $K_{ev0}$ and $K_{es0}$ are identified as 770 kPa and 1155 kPa, respectively when the average confined stress $p_0=4$ kPa. Based on the following relationships:

$$K = K_{ev0}\frac{p'}{p_0}, \quad G = K_{es0}\frac{p'}{3p_0},$$
$$\mu = \frac{3K-2G}{2(3K)}, \quad E = 2G(1+\mu), \tag{7}$$

where $p'$ is the confined stress in soil at a position. Obviously, $p'$ is not a constant in soil. $K$ is the bulk modulus. To simulate the seismic dynamics of the clayed sand embankment and the Nevada loose sand foundation adopting the developed 3D FEM program by using elastic model, constant Young's modulus $E$ and Poisson's ratio $\mu$ of the embankment and foundation need to be estimated based on the above mentioned parameters and relationships by taking an appropriate average confined pressure $p'$ for the embankment and foundation. Finally, the Young's modulus of the embankment and foundation are estimated as 13.6 MPa and 8 MPa, respectively; and the Poisson's ratio of the embankment and foundation are estimated as 0.2857 and 0.3101 for the numerical computation, respectively.

Fig. 3 illustrates the comparison between the numerical results and experimental acceleration data [19]. As shown in Fig. 3, an overall agreement between the numerical results and experimental data is observed. The deviation between numerical results and experimental data may mainly be attributed to the identification of parameters used in the computation.

### 2.2. Boundary conditions

The computational domain chosen is a large scale seabed-breakwater model. The size of seabed is 370 m × 370 m × 30 m (length × width × thickness); and a rubble mound breakwater (length=220 m, bottom width=53 m, height=16 m, slope gradient=2:3) is built on the seabed. Boundary conditions used in computation are outlined here:

(1) The bottom of seabed is considered as rigid and impermeable

$$\frac{\partial p_s}{\partial z} = 0 \quad \text{at } z = 0. \tag{8}$$

(2) The front and rear lateral sides of the seabed, and the end side of the rubble mound breakwater are also impermeable

$$\frac{\partial p_s}{\partial y} = 0 \quad \text{at } y = 0 \text{ and } y = 370 \text{ m}. \tag{9}$$

(3) The hydrostatic pressure is applied on the surface of a the seabed and the outer surface of the rubble mound breakwater. All hydrostatic forces are perpendicular with the surfaces (Fig. 4). The consideration of the hydrostatic pressures in seismic analysis is necessary because that the application of the hydrostatic pressure on the seabed and the rubble mound breakwater could significantly change the natural frequency of the seabed and the rubble mound breakwater [7]. It will further affect the resonance phenomenon of marine structures. It is noted that the effect of the vibrated seabed foundation and marine structures on the static water level is not considered in this study. The vibrated seabed and marine structures could lead to the generation of small wave in sea water. The previous experiments indicates that the dynamic pressure acting on the seabed and the rubble mound breakwater induced by the small wave generally only accounts for a small percentage of the total pressure [7].

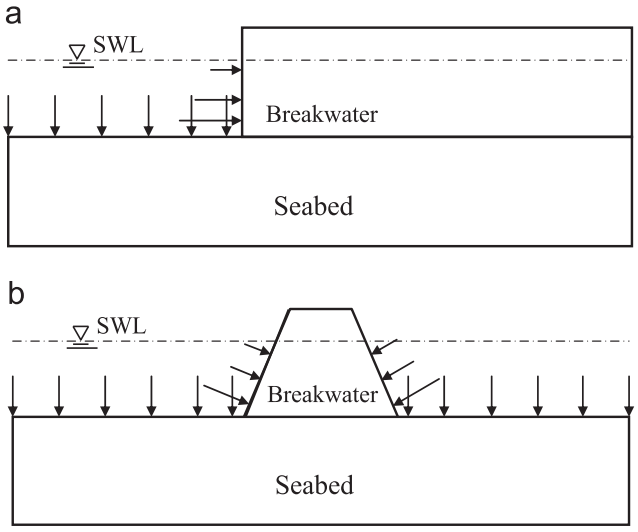


**Fig. 4.** The schematic map of hydrostatic pressure acting on the rubble mound breakwater and seabed. (a) Section $x=180$ m. (b) Section $y=276.5$ m.

(4) The seismic accelerations in three directions (E–W, N–S and U–D (vertical)) are applied to the four lateral sides and the bottom of computational domain simultaneously. In this study, the acceleration in E–W, N–S and U–D direction are applied to the $x$-, $y$- and $z$-direction respectively.

$$\begin{cases} (a_x)_t = (a_{EW})_t \\ (a_y)_t = (a_{NS})_t \\ (a_z)_t = (a_{UD})_t \end{cases} \quad \text{on four lateral sides and bottom} \tag{10}$$

where $(a_x)_t$, $(a_y)_t$ and $(a_z)_t$ are the accelerations in the $x$-, $y$- and $z$-directions on lateral sides and bottom of computational domain at time $t$. $(a_{EW})_t$, $(a_{NS})_t$ and $(a_{UD})_t$ are the input seismic acceleration at E–W, N–S and U–D (vertical) directions at time $t$. Such an application of seismic acceleration to the boundaries of computational domain is similar to that in shaking table tests and centrifuge tests. This method could effectively avoid the generation of reflected wave in a seismic analysis. Otherwise, the viscous absorbing boundary has to be used if the seismic wave is the only input at the bottom of the seabed foundation in numerical simulation [11]. In the process of seismic waves propagation, the chosen computational domain may be insufficient to ensure the attenuation of seismic waves, when it passes through the seabed foundation. Therefore, it is reasonable to apply the same seismic wave to each lateral side and the bottom of the seabed foundation at each analysis time step [15,18].

In general, the seabed foundation under a rubble mound breakwater has been consolidated before the seismic wave arriving. The consolidation status of the seabed foundation under the rubble mound breakwater should be taken as the initial condition for the earthquake analysis. The consolidation of the seabed foundation under the rubble mound breakwater and hydrostatic pressure is firstly determined. Taking the final consolidation status as the initial condition, the seismic responses of the seabed foundation and the rubble mound breakwater are then investigated.

It is noted that the hydrodynamic loading on a marine structure during an earthquake event is not considered in this study. In fact, except the extreme cases such as tsunamis, the

hydrodynamic loading is much less than the seismic loading during an earthquake event. Furthermore, the dynamic wave pressure amplitude is much smaller than the hydrostatic water pressures. Therefore, we ignore the hydrodynamic loading in this study. To include the effects of extremely hydrodynamic loading (i.e., tsunamis), hydrodynamic model for tsunamis are required. However, the existing wave models for tsunami waves can only predict the wave characteristics for the wave propagation, but not during the earthquake loading. For the combined tsunamis and earthquake loadings, there is no hydrodynamic model available.

## 3. Earthquake input data

In this study, the seismic waves induced by the Japan 311 off the pacific coast of Tohoku earthquake ($M_L$ magnitude=9.0) is used as the earthquake loading to apply the dynamic loading to the seabed foundation and rubble mound breakwater. To apply a strong seismic loading to the seabed foundation, the seismic wave of accelerations recorded at a place where near to the epicenter of earthquake and located near coastline is chosen as the input seismic accelerations in computation.

The seismic wave recorded at the observation station labeled as MYGH03 (located at 141.6412E, 38.9178N) is chosen as the input earthquake loading (provided by National Research Institute for Earth Science and Disaster Prevention (NIED) in Japan). The distance from this chosen observation station to the epicenter (142.9E, 38N) is 154 km (Fig. 5(a)); and this observation station is near the coastal line of pacific ocean (Fig. 5(b)). Therefore, the chosen input seismic acceleration wave in this study is similar as close as possible with the real seismic wave propagating to the seabed foundation.

There are two types of seismic waves recorded at observation station MYGH03. One is recorded on ground and the other is recorded at the position underground. Undoubtedly, the seismic wave recorded on ground is significantly affected by the site conditions. The acceleration recorded generally is amplified by the soil layers. However, the seismic acceleration wave recorded underground is not affected by the site conditions. Therefore, the seismic acceleration wave recorded underground is used in this study (Fig. 6). It is found in Fig. 6 that the seismogenic fault in the subduction zone of pacific plate dislocates two times in the earthquake event. The vibration induced by the first dislocation is stronger than that induced by the second dislocation. The maximum acceleration in E–W, N–S and U–D (vertical) direction are 133.2 cm/s$^2$, 153.7 cm/s$^2$ and 121.7 cm/s$^2$, respectively. The duration of this strong earthquake is about 200 s (from 25 s to 225 s).

## 4. Results and discussion

In this section, the dynamic responses of a rubble mound breakwater and its seabed foundation under the strong earthquake loading are investigated. The properties of the seabed foundation and the rubble mound breakwater are listed in Table 1. It is noted that an unsaturated seabed is considered in this study. It is not uncommonly to have unsaturated seabed in the real marine environments. Numerous evidences have been reported in the field study [20–22]. It is reported that the in site degree of saturation of marine sediments normally lies in the range of 85% to 100%. There are air bubbles, methane more or less in the seabed soil. Some previous models have limited their models to the saturated soils mainly because of that their models cannot consider the non-saturation of soil. The compressibility of pore water in an unsaturated soil is significantly different from that in a fully saturated soil. The three-dimensional iso-parametric brick element with 27 nodes is used to discrete the computational domain, which is the complete third-order element, deserving highly accurate results.

### 4.1. Response of rubble mound breakwater

It is assumed that a rubble mound breakwater is built on the seabed in the offshore environment near to the observation station MYGH03. In this section, the dynamic response of a rubble mound breakwater to the Japan 311 off pacific coast of Tohoku earthquake ($M_L$ magnitude=9.0) is studied. The dynamic response of a series of points on the rubble mound breakwater is monitored in the seismic analysis. The coordinates of these points (B1–B7) are shown in Fig. 7. Herein, the point B1 (274 m, 150 m, 46 m) which locates at the top corner of the head of rubble mound breakwater is chosen as the representative position for the investigation of the dynamic response of a rubble mound breakwater.

Figs. 8–10 illustrate the historic curves of dynamic response of acceleration, velocity and displacement of the rubble mound breakwater at position B1 under the strong earthquake loading. As shown in Fig. 8, the maximum acceleration in E–W, N–S and

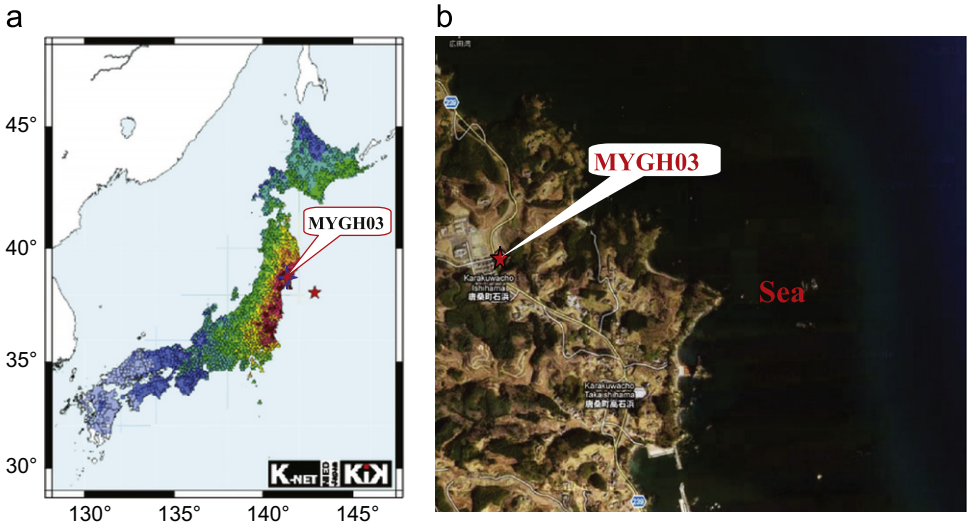


**Fig. 5.** The position of the observation station MYGH03 (installed by NIED in Japan). It locates at the point (141.6412E, 38.9178N) near to the east coast of Japan.

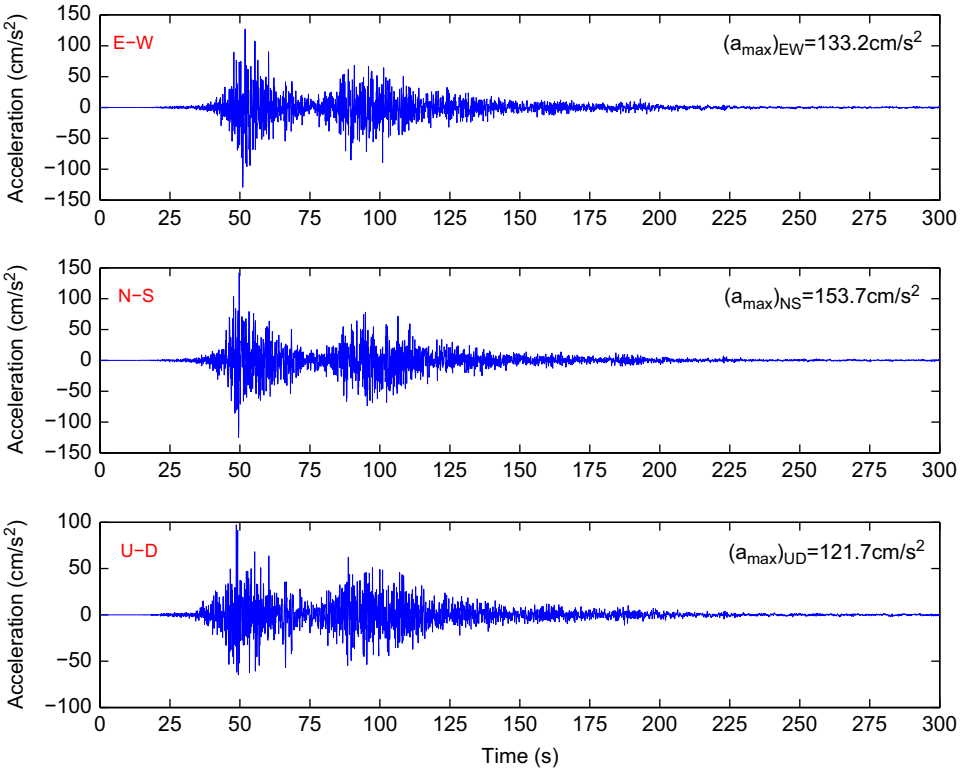


**Fig. 6.** The input seismic acceleration wave recorded at observation station MYGH03 in the Japan 311 off the pacific coast of Tohoku earthquake ($M_L$ magnitude=9.0).

**Table 1**
Properties of sandy seabed and the rubble mound breakwater adopted in calculation.

| Object | $G$ (N/m$^2$) | $\mu$ | $S_r$ (%) | $k$ (m/s) | $n$ | Special gravity |
|---|---|---|---|---|---|---|
| Seabed | $6.0\times10^7$ | 0.3333 | 98 | $1.0\times10^{-4}$ | 0.3 | 2.65 |
| Breakwater | $1.0\times10^9$ | 0.25 | 100 | $2.0\times10^{-1}$ | 0.35 | 2.65 |

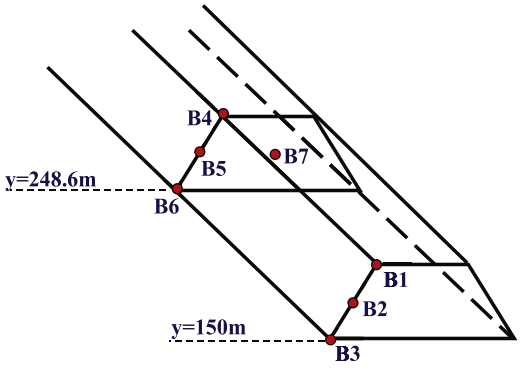


**Fig. 7.** The positions of points B1–B7 on/in the rubble mound breakwater. Coordinates of points: B1: (274, 150, 46); B2: (267, 150, 37.5); B3: (250, 150, 30); B4: (274, 248.6, 46); B5: (267, 248.6, 37.5); B6: (250, 248.6, 30); B7: (276.5, 248.6, 35.5).

U–D direction at B1 is 8.46 m/s$^2$, 4.39 m/s$^2$ and 3.57 m/s$^2$. Compared with the maximum input acceleration in the three directions, it is found that the accelerations are amplified greatly when the seismic wave propagating in a porous seabed and rubble mound breakwater. The magnification of the response acceleration at B1 in E–W, N–S and U–D direction is 6.35, 2.86 and 2.93 respectively. It indicates that the horizontal acceleration in E–W direction is amplified most strongly relative to the amplification in other two directions. This could be attributed to the configuration of the rubble mound breakwater. The rubble mound breakwater is built along the $y$-axis (N–S direction). In the E–W ($x$) direction, the rubble mound breakwater is relatively small ($x$=250–303 m), and the two lateral sloped sides are free to vibrate. The rubble mound breakwater is relatively large ($y$=150–370 m) in the N–S ($y$) direction, and the end of the breakwater ($y$=370 m) is fixed in $y$-direction. The gravity of a rubble mound breakwater and a seabed undoubtedly could prevent the vertical input seismic acceleration from amplifying significantly.

As illustrated in Figs. 9 and 10, the maximum response velocities and displacements at B1 in the E–W, N–S and U–D direction are 1.59 m/s, 0.646 m/s, 0.286 m/s and 32.28 cm, 13.83 cm 5.94 cm respectively. It indicates that the dynamic response in E–W direction is much more intensive than that in other two directions.

The maximum response accelerations, velocities and displacements on the six points (B1 to B6) are listed in Table 2. Among these six points, B1 to B3 are located at the head of rubble mound breakwater ($y$=150 m); B4 to B6 are located at the middle part of the rubble mound breakwater ($y$=248.6 m). As illustrated in Table 2, it is found that the dynamic response at the head and the middle part of the rubble mound breakwater is a little different. Furthermore, the rubble mound breakwater basically has not amplified the dynamic response from its bottom to its top on the same section. It is found that the amplification effect mainly attributes to the porous seabed. The obvious difference of dynamic response at the head and at the middle part of the breakwater is that the maximum response accelerations in N–S and U–D directions at the head of breakwater are much greater than that at the middle part of breakwater.

Fig. 11 shows the dynamic response of pore pressure in the rubble mound breakwater at point B7 (276.5 m, 248.6 m, 35.5 m,

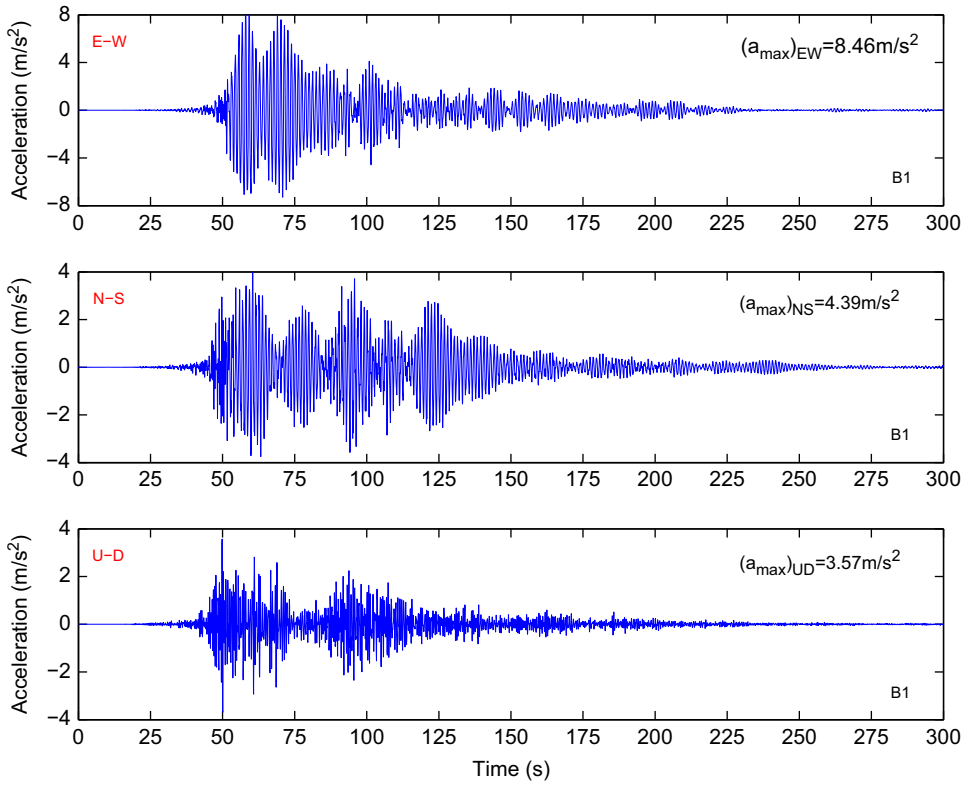


**Fig. 8.** The response of acceleration of the rubble mound breakwater at position B1 (274 m, 150 m, 46 m).

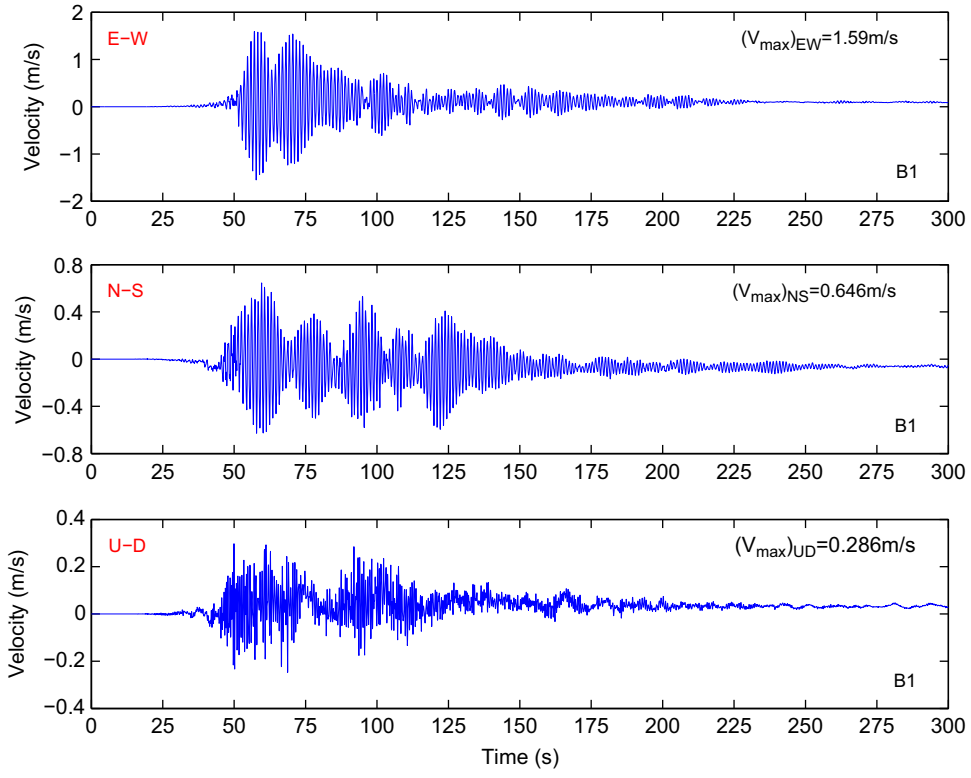


**Fig. 9.** The response of velocity of the rubble mound breakwater at position B1 (274 m, 150 m, 46 m).

in the rubble mound breakwater). As mentioned in the previous section, the small wave generated by the vibration of the seabed foundation and the rubble mound breakwater is not taken into consideration. As illustrated in Fig. 11, there is no any excess pore pressure at B7 before the seismic wave arriving at the seabed foundation. After the seismic wave arriving, the pore pressure at

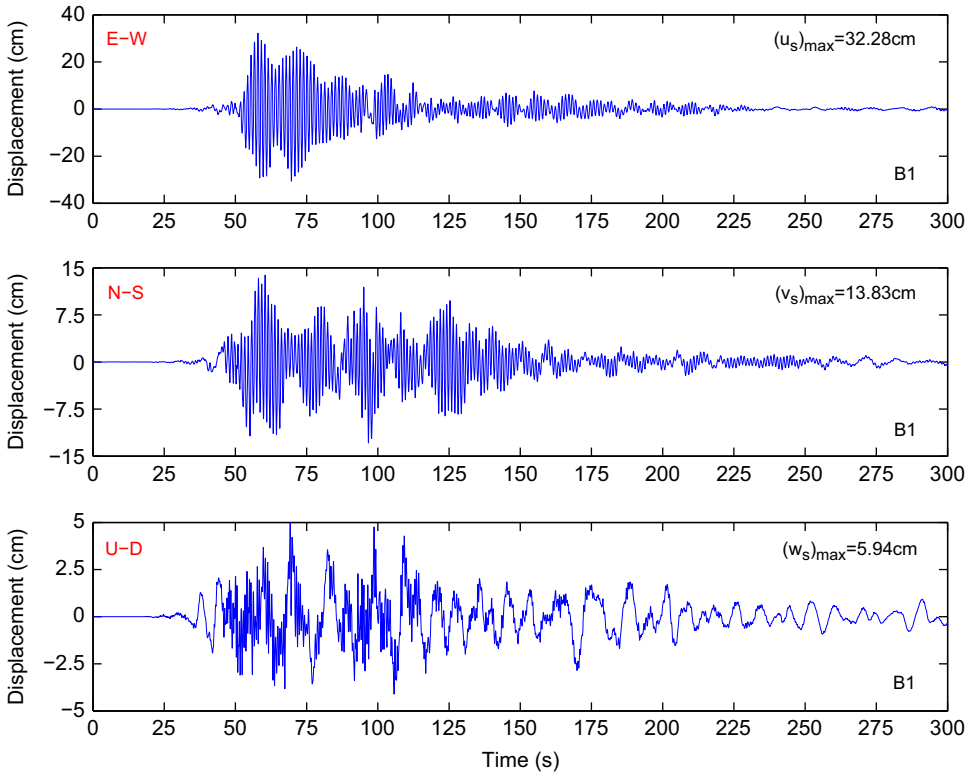


**Fig. 10.** The response of displacement of rubble mound breakwater at position B1 (274 m, 150 m, 46 m).

**Table 2**
The coordinates of chosen points on rubble mound breakwater, and their maximum dynamic response of acceleration, velocity and displacement (Notice: all points are on the left lateral sloped side of rubble mound breakwater).

| Point | B1 | B2 | B3 | B4 | B5 | B6 |
|---|---|---|---|---|---|---|
| $x$ (m) | 274 | 267 | 250 | 274 | 267 | 250 |
| $y$ (m) | 150 | 150 | 150 | 248.6 | 248.6 | 248.6 |
| $z$ (m) | 46 | 37.5 | 30 | 46 | 37.5 | 30 |
| Acceleration | | | | | | |
| $a_{EW}$ (m/s$^2$) | 8.59 | 8.16 | 7.64 | 9.34 | 8.90 | 8.37 |
| $a_{NS}$ (m/s$^2$) | 4.39 | 4.89 | 4.89 | 2.92 | 2,68 | 2.61 |
| $a_{UD}$ (m/s$^2$) | 3.57 | 2.99 | 3.06 | 1.97 | 1.91 | 2.90 |
| Velocity | | | | | | |
| $v_{EW}$ (m/s) | 1.59 | 1.55 | 1.36 | 1.71 | 1.70 | 1.65 |
| $v_{NS}$ (m/s) | 0.65 | 0.76 | 0.84 | 0.46 | 0.47 | 0.49 |
| $v_{UD}$ (m/s) | 0.29 | 0.25 | 0.25 | 0.19 | 0.20 | 0.22 |
| Displacement | | | | | | |
| $d_{EW}$ (cm) | 32.27 | 31.63 | 28.85 | 35.74 | 35.11 | 33.45 |
| $d_{NS}$ (cm) | 13.83 | 15.57 | 17.42 | 11.15 | 11.50 | 11.65 |
| $d_{UD}$ (cm) | 5.94 | 5.62 | 4.30 | 4.77 | 4.54 | 4.21 |

B7 begins to vibrate, and generate the excess pore pressure in the rubble mound. Due to the fact that the rubble mound breakwater is considered as elastic medium, there is no residual pore pressure generated in the rubble mound breakwater, only oscillatory pressure exists. The maximum earthquake-induced excess pore pressure reaches up to 17.7 kPa, equivalently 1.8 m water height difference.

In offshore engineering, the response spectrums of marine structures to an earthquake which probably occurs nearby the site of seabed foundation are one of important factors for the structure design. In general, coastal engineers attempt to design marine structures to avoid the occurrence of resonance when an earthquake occurs. The method is that the weight and shape of marine structures is designed and controlled, making the natural frequency of marine structures is different from the dominant frequency of seismic waves. On the other hand, if the natural frequency of a marine structure is known, the fortification acceleration for the marine structure against the earthquake-induced failure can be determined from the acceleration response spectrum.

Fig. 12 illustrates the response spectrum of accelerations, velocities and displacements of a rubble mound breakwater to the strong earthquake loading (damping ratio=5%, widely used in structure design). From Fig. 12, it can be seen that the resonance of a rubble mound breakwater would occur at the E–W, N–S directions, and U–D directions, if the natural frequency of the rubble mound breakwater is about 1.2 s and 0.45 s. Therefore, the natural frequency of the rubble mound breakwater has to be controlled to be out of the range of 0.4 s–0.5 s and 1.0 s–2.0 s in design. It is suggested that the natural frequency of the rubble mound breakwater is less than 0.4 s or greater than 2.0 s. Then, the dynamic response of a rubble mound breakwater to the strong earthquake loading could be controlled to be as little as possible. As illustrated in Fig. 8, the maximum E–W acceleration of the rubble mound breakwater at B1 is 8.59 m/s$^2$, nearly 0.88$g$. Accordingly, the fortification acceleration for this rubble mound breakwater in this strong earthquake event should not be less than 0.9$g$. In engineering practice, it is difficult or costly to design a structure to defense an acceleration which is greater than 0.9$g$. Therefore, the marine structures constructed near to the epicenter are most likely to fail in the strong earthquake events.

### 4.2. Response of porous seabed

As a kind of natural foundation for marine structures, the dynamic response of seabed foundation to seismic waves propagating through the porous seabed is one of key factors to be considered for the prevention of earthquake-induced failure. The engineers must make an evaluation of seismic security for the sites of foundation, to determine whether the chosen sites is

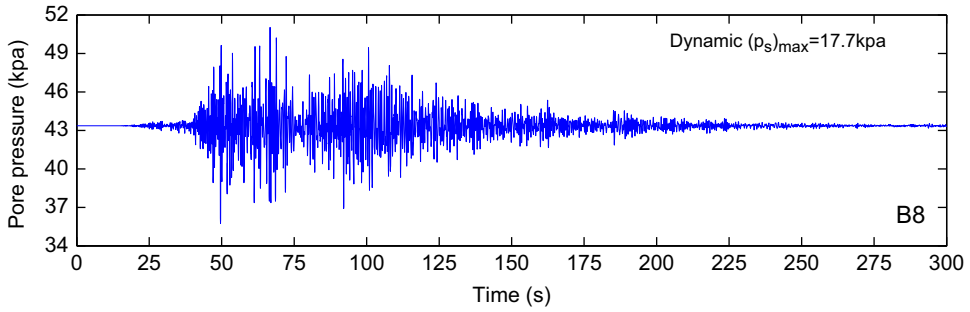


**Fig. 11.** The dynamic response of pore pressure in rubble mound breakwater at point B7 (276.5 m 248.6 m 35.5 m).

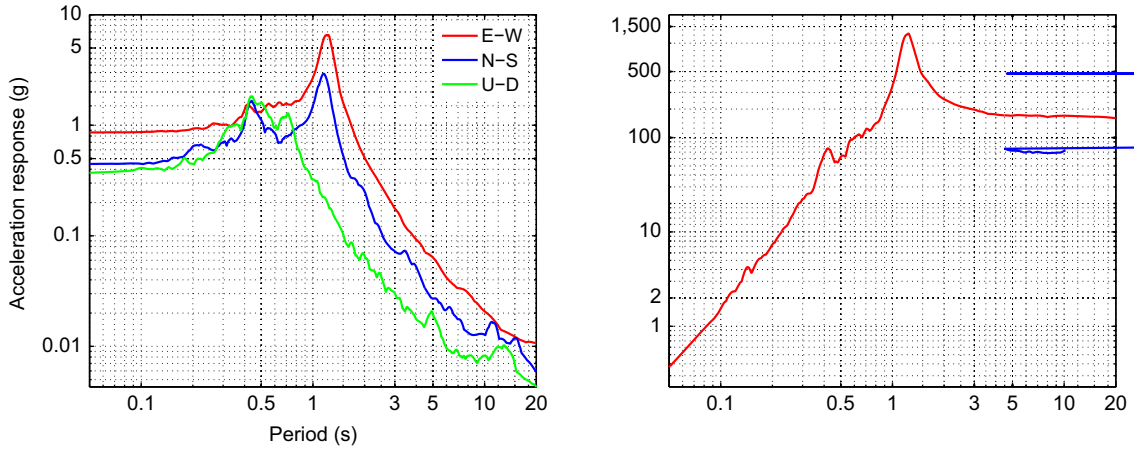


suitable for the construction of a marine structure. If a marine structure is decided to construct on a site foundation, the engineers have to determine the fortification acceleration for the structures design according to the dynamic response (such as response spectrums) of the chosen seabed foundation to a seismic wave. In this section, the response of a porous seabed foundation under the rubble mound breakwater to the Japan 311 off pacific coast of Tohoku earthquake is investigated. Three representative positions S15 (276.5 m, 248.6 m, 28 m), S14 (276.5 m, 248.6 m, 5.6 m) and P2 (238.3 m, 170 m, 29 m) in the seabed are chosen to illustrate the response of a seabed foundation. S15 and S14 are under the rubble mound breakwater; and S15 is just above S14. P2 is located at the left side of the rubble mound breakwater, and near to the seabed surface.

Figs. 13–15 present the dynamic response of accelerations, velocities and displacements of the seabed foundation at position S15. The maximum response acceleration in E–W, N–S and U–D direction at S15 is 8.61 m/s$^2$, 2.78 m/s$^2$ and 1.85 m/s$^2$ respectively. Meanwhile, they are 2.67 m/s$^2$, 1.94 m/s$^2$ and 0.906 m/s$^2$ in E–W, N–S and U–D direction at S14. Comparing the maximum response acceleration at S15 and S14 with the input maximum acceleration in the three directions, it is found that: (1) The response of the seabed foundation in E–W direction is strongest among the three directions. (2) The porous seabed foundation amplifies significantly the seismic waves propagating in it. (3) The amplification effect of a porous seabed to the seismic wave is mainly related to the depth of position; the amplification is most obvious at the surface of a seabed foundation. This is consistent with the experimental results in [6]. The maximum response velocity and displacement at S15 and S14 (listed in Table 3) could further confirm the above three conclusions. In engineering practice, the amplification effect of porous seabed foundation to

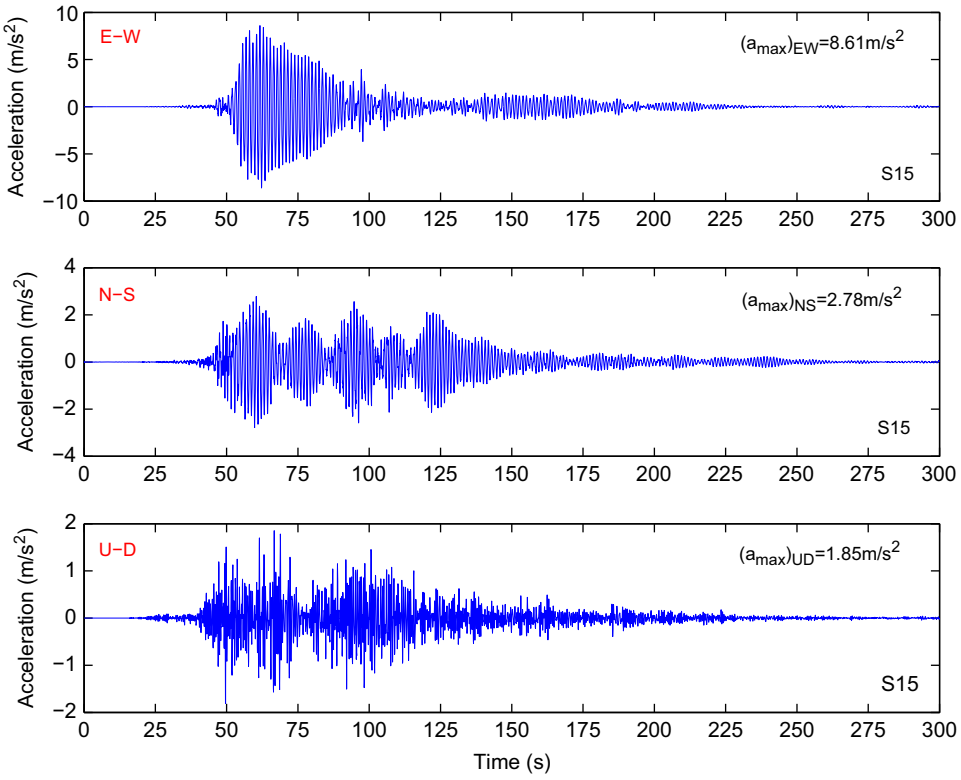


**Fig. 13.** The acceleration response of porous seabed foundation at position S15.

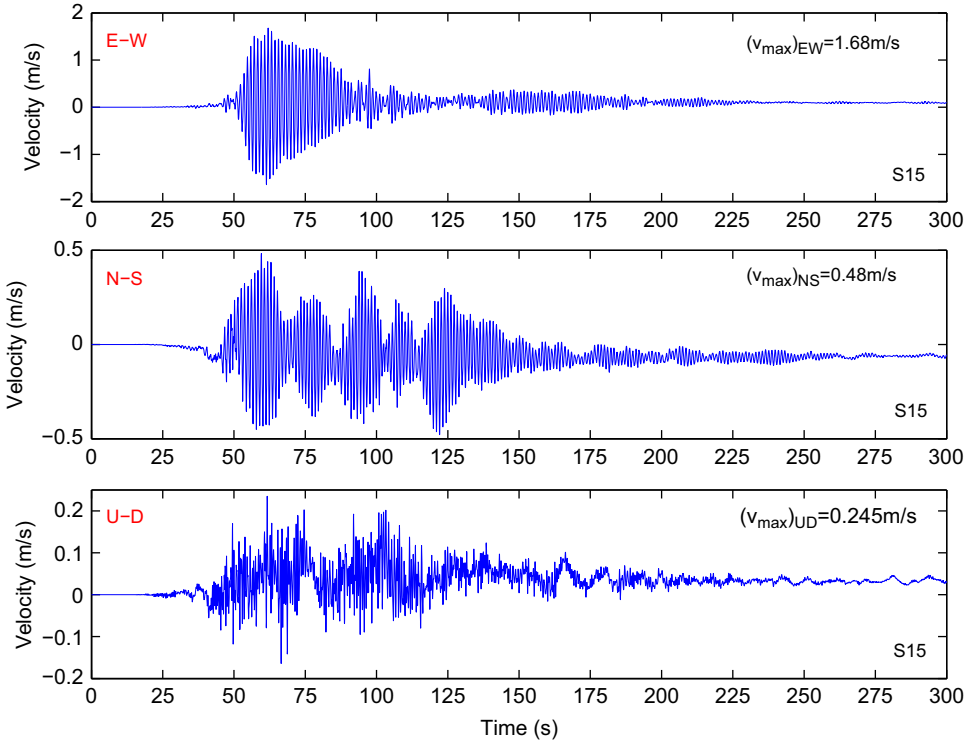


**Fig. 14.** The velocity response of porous seabed foundation at position S15.

seismic wave is an unfavorable factor for the stability of marine structures.

Fig. 16 illustrates the dynamic response of pore pressure in the seabed foundation at position S15. As shown in Fig. 16, the pore pressure at S15 oscillates with a large amplitude under the loading of strong earthquake, and generates the excess pore pressure at S15. The maximum excess pore pressure reaches up to 19.5 kPa, equivalently 1.99 m water height difference. At position S14, the pore pressure also oscillates similarly with that at position S15. The maximum excess pore pressure is 41.5 kPa (4.23 m water height difference). It could be concluded that the earthquake-induced excess pore pressure in a seabed foundation

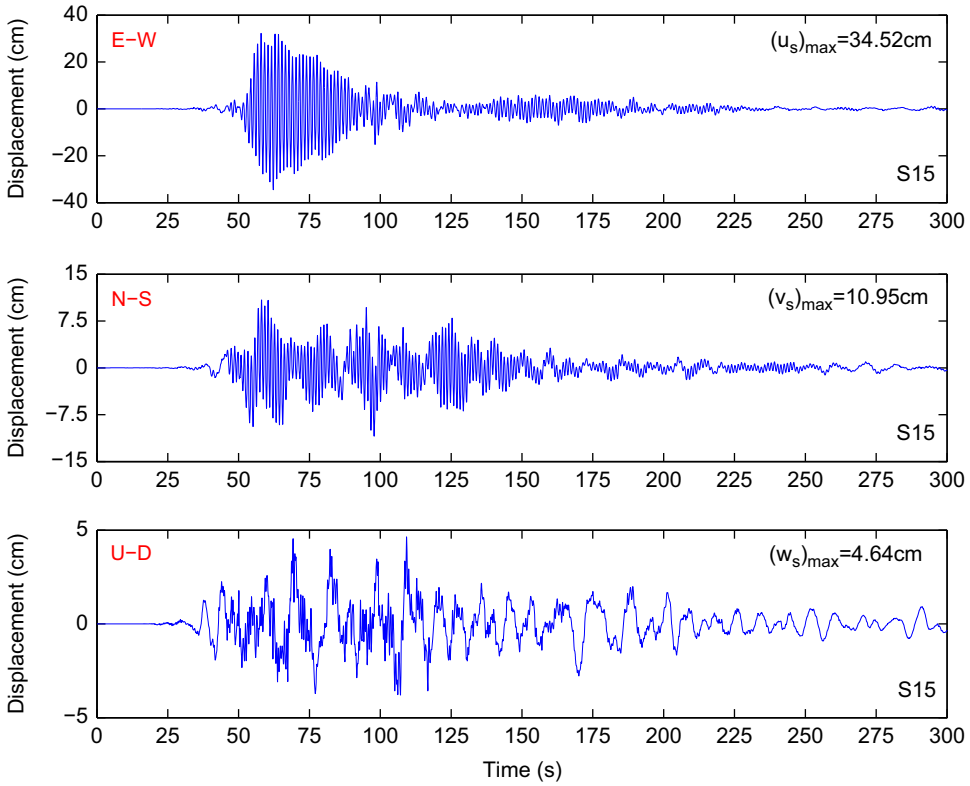


**Fig. 15.** The displacement response of porous seabed foundation at position S15.

**Table 3**
The coordinates of S15, S14, and their maximum dynamic response of acceleration, velocity and displacement.

| Point | S15 | S14 |
|---|---|---|
| $(x, y, z)$ m | (276.5, 248.6) | (276.5, 248.6) |
| Acceleration | | |
| $a_{EW}$ (m/s$^2$) | 8.61 | 2.67 |
| $a_{NS}$ (m/s$^2$) | 2.78 | 1.94 |
| $a_{UD}$ (m/s$^2$) | 1.85 | 0.91 |
| Velocity | | |
| $v_{EW}$ (m/s) | 1.68 | 0.4759 |
| $v_{NS}$ (m/s) | 0.48 | 0.1874 |
| $v_{UD}$ (m/s) | 0.245 | 0.145 |
| Displacement | | |
| $d_{EW}$ (cm) | 34.52 | 10.44 |
| $d_{NS}$ (cm) | 10.95 | 6.95 |
| $d_{UD}$ (cm) | 4.6 | 4.0 |

is positively related to the buried depth. The earthquake-induced excess pore pressure increases with the depth. This finding is consistent with the results reported in [10]. Although the excess pore pressure in the region near the bottom of seabed foundation is greater, the soil in the bottom region is difficult to be liquefied due to that the upward seepage force cannot overcome the weight of the overlying soil. Liquefaction only occurs in the region near to the surface of porous seabed. In this study, what we investigate is a poro-elastic seabed foundation. Therefore, there is no built-up of the pore pressure in the seabed foundation. The build-up of pore pressure under seismic loading will be further investigated adopting elasto-plastic models in the future.

It has been recognized that the shear failure of seabed foundation mainly depends on the shear stress $\tau_{xz}$ developed in seabed near to the rubble mound breakwater; and the liquefaction of porous seabed is significantly affected by the dynamic vertical effective stress $\sigma'_z$ developed in seabed. Due to the fact that the point S15 is located at the symmetrical plane $x=$ 276.5 m, the shear stress $\tau_{xz}$ at S15 is always near zero, and the seabed under the rubble mound breakwater cannot liquefy because of the compression of marine structures.

Another position P2 (238.33 m, 170 m, 29 m) is chosen as the representative to investigate the dynamic response of effective stresses under the strong earthquake loading (The Japan 311). P2 is located at the left side of the rubble mound breakwater. Fig. 17 shows the dynamic response of the vertical effective stress $\sigma'_z$ and $\tau_{xz}$ at P2 to the strong earthquake loading. It can be seen that the maximum dynamic $\sigma'_z$ is 31.1 kPa. When the strong seismic wave induced by the Japan 311 off pacific coast of Tohoku earthquake goes through the seabed foundation ($t=$50 s–100 s), the transient tensile vertical effective stress appears at position P2. In this period ($t=$50 s–100 s), the transient liquefaction occurs at P2 (the transient liquefaction occurs when the upward seepage force can overcome the overburdened soil weight). Meanwhile, the maximum dynamic shear stress $\tau_{xz}$ in 50 s–100 s reaches up to 24.1 kPa at P2. This great dynamic shear stress $\tau_{xz}$ developed due to the strong earthquake loading would lead to the shear failure in the seabed foundation. In engineering design, the liquefaction and shear failure induced by the probable strong earthquake loading are suggested to be evaluated before the marine structures are constructed.

Fig. 18 illustrates the response spectrum of acceleration, velocity and displacement of a seabed foundation to the Japan 311 off pacific coast of Tohoku earthquake. These response spectrums could provide very important basis for the design of a rubble mound breakwater which would suffer from a strong earthquake in its usage life. From the response spectrums of a seabed foundation, the engineers can take measurements to avoid the natural frequency of marine structures approaching the dominant frequency of seismic wave; and can determine the fortification acceleration for marine structures to against the earthquake damage. It is suggested that the natural frequency

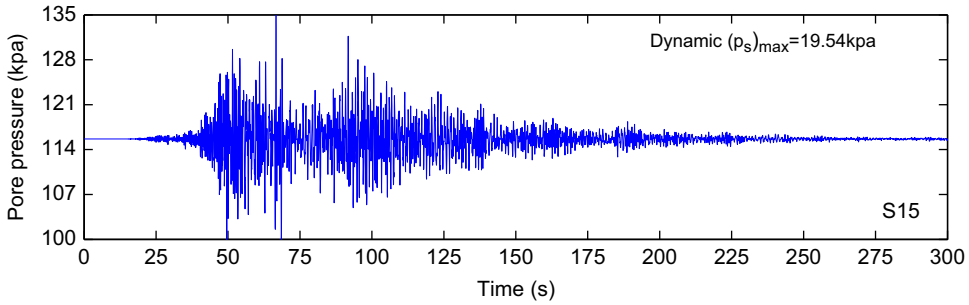


**Fig. 16.** The dynamic response of pore pressure in porous seabed foundation at position S15.

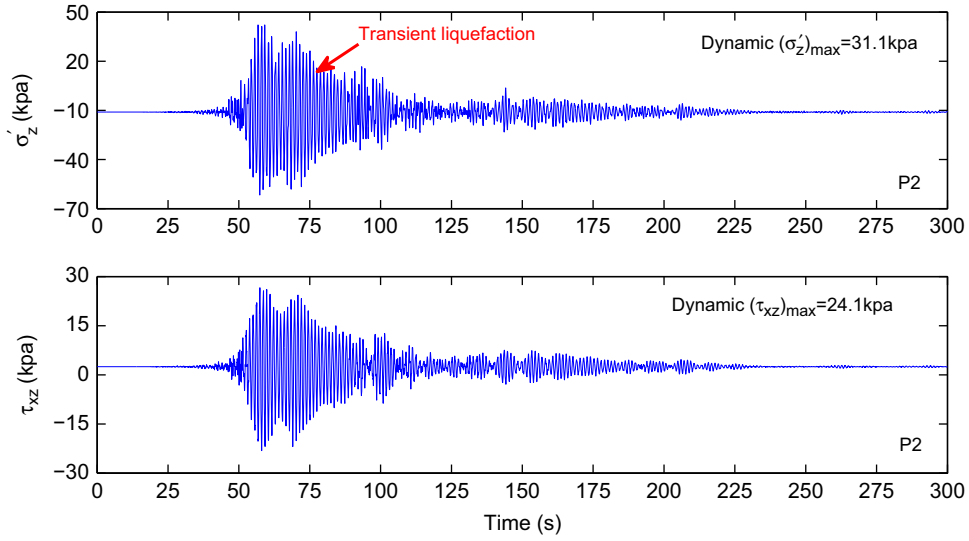


**Fig. 17.** The dynamic response of vertical effective stress $\sigma_z'$ and $\tau_{xz}$ in seabed at position P2 (238.33 m, 170 m, 29 m).

of rubble mound breakwater is less than 0.4 s or greater than 2.0 s. The corresponding fortification acceleration could be 0.9*g* or 0.1*g*–0.3*g*.

## 5. Conclusions

In this study, based on Biot's dynamic poro-elastic theory, the dynamic response of a rubble mound breakwater and its seabed foundation to a strong seismic loading is investigated, with the case study of the Japan 311 off pacific coast of Tohoku earthquake. The input seismic wave used in this study is the record monitored by the seismic observation station MYGH03, which is near the epicenter (142.9E, 38.0N). The distance from the observation station to the epicenter is 154 km. Based on the analysis results, the following conclusions can be drawn:

(1) The dynamic response of a rubble mound breakwater to the strong earthquake loading is significant. The maximum acceleration in E–W, N–S and U–D direction reaches up to 8.46 m/s$^2$, 4.39 m/s$^2$ and 3.57 m/s$^2$ respectively. The maximum of magnitude of vibration of the breakwater is 32.27 cm in the E–W direction.

(2) The amplification effect of acceleration is insignificant in the rubble mound breakwater. However, the porous seabed can amplify the seismic wave greatly; and the amplification of acceleration in E–W direction is greater than that in N–S and U–D direction. It also could be observed that the amplification of seismic wave is negatively related to the depth. There is no amplification at the bottom of a seabed foundation. The amplification is greatest on the surface of a seabed foundation. The amplification of acceleration could reach up to 6.35 times of the maximum input acceleration at the surface of the seabed foundation in E–W direction.

(3) The response spectrums of acceleration, velocity and displacement have been obtained in the earthquake analysis. The response spectrums could provide the coastal engineers with valuable information in the structure design. On the one side, the occurrence of resonance should be avoided for marine structures. On the other side, the fortification acceleration against the earthquake-induced failure could be determined based on the response spectrum of acceleration.

(4) In this study, the relative displacement of pore water to solid matrix is ignored in the governing equations. This assumption may be not applicable in the outer surface zone (armour layer) of the rubble mound breakwater, because the relative displacement of pore water in the zone could be great, if the earthquake-induced water wave in the fluid domain is relatively huge. In future, a fluid numerical model can be integrated into the 3D FEM program through the displacement continuity at the interface between solid domain and fluid domain, to investigate the motion of seismic wave induced water wave near to the rubble mound breakwater; and the 3D FEM program can be further developed to include the term of relative displacement of pore water to solid matrix.

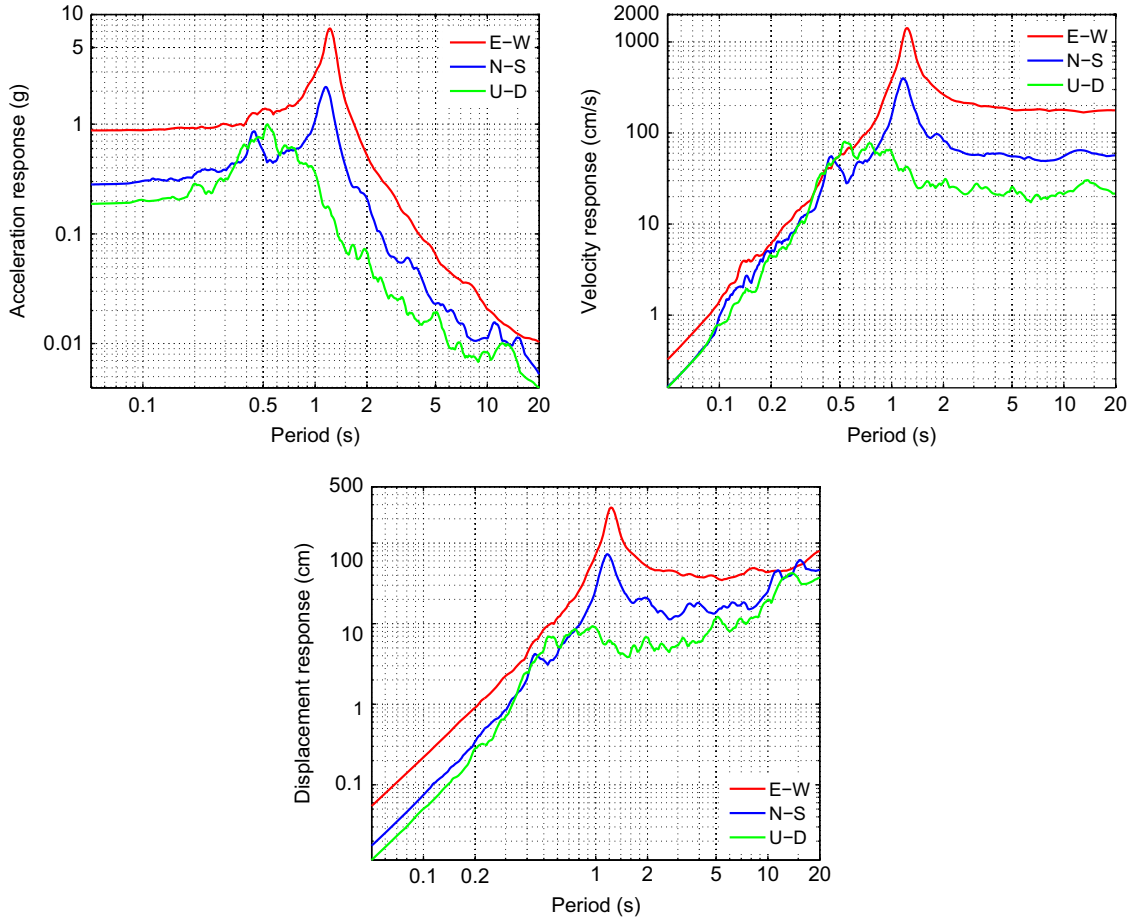


**Fig. 18.** The response spectrum of acceleration, velocity and displacement of seabed foundation to the Japan 311 off pacific coast of Tohoku earthquake.

## Acknowledgments

The authors are grateful for the financial support from EPSRC #EP/G006482/1.

## References

[1] Iai S, Kameoka T. Finite element analysis of earthquake induced damage to anchored sheet pile quay walls. Soils and Foundation 1993;33(1):71–91.
[2] Sugano T, Kaneko H, Yamamoto S. Damage to port facilities. The 1999 Ji–Ji earthquake, Taiwan, investigation into the damage to civil engineering structures. Journal of Japanese Society of Civil Engineering 1999:51–7.
[3] Sumer BM, Kaya A, Hansen NEO. Impact of liquefaction on coastal structures in the 1999 Kocaeli, Turkey earthquake. In: Proceedings of the international offshore and polar engineering conference, vol. 12. 2002. p. 504–11.
[4] Yuksel Y, Cetin KO, Ozguven O, Isik NS, Cevik E, Sumer BM. Seismic response of a rubble mound breakwater in Turkey. Proceedings of the Institution of Civil Engineers: Maritime Engineering 2004;157(4):151–61.
[5] Jeng DS. Wave-induced sea floor dynamics. Applied Mechanics Review 2003;56(4):407–29.
[6] Kiara A, Memos C, Tsiachris A. Some practical aspects on the seismic behavior of rubble-mound breakwaters. In: Ports 2001: America's ports – gateways to the global economy – proceedings of the ports 2001 conference, vol. 108, 2004. p. 1–10.
[7] Memos C, Bouckovalas G, Tsiachris A. Stability of rubble-mound breakwaters under seismic action. In: Coastal engineering 2000 – proceedings of the 27th international conference on coastal engineering, ICCE 2000, vol. 276, 2000. p. 1585–98.
[8] Westergaard HM. Water pressure on dams during earthquakes. Transaction ASCE 1993;98(2):418–33.
[9] Liu YK, Zhu T. Investigation of seismic response and stability of breakwaters under seepage flows. In: Proceedings of the international offshore and polar engineering conference, vol. 3, 2001. p. 559–63.
[10] Memos CD, Kiara A, Pavlidis E. Coupled seismic response analysis of rubble-mound breakwaters. Proceedings of the Institution of Civil Engineers: Water and Maritime Engineering 2003;156(1):23–31.
[11] Jafarian Y, Alielahi H, Abdollahi AS, Vakili B. Seismic numerical simulation of breakwater on a liquefiable layer: Iran LNG portElectronic Journal of Geotechnical Engineering 2010;15(D):1–11.
[12] Byme P. A cyclic shear–volume coupling and pore-pressure model for sand. In: Second international conference on recent advances in geotechnical earthquake engineering and soil dynamics, vol. 1.24, 1991. p. 47–55.
[13] Cihan K, Yuksel Y. Deformation of rubble-mound breakwaters under cyclic loads. Coastal Engineering 2011;58(6):528–39.
[14] Zienkiewicz OC, Chang CT, Bettess P. Drained, undrained, consolidating and dynamic behaviour assumptions in soils. Geotechnique 1980;30(4):385–95.
[15] Chan AHC. A unified finite element solution to static and dynamic problems of geomechanics. PhD thesis, University of Wales, Swansea Wales; February 1988.
[16] Zienkiewicz OC, Chan AHC, Pastor M, Schrefler BA, Shiomi T. Computational Geomechanics with Special Reference to Earthquake Engineering. England: John Wiley & Sons; 1999.
[17] Biot MA. Theory of propagation of elastic waves in a fluidsaturated porous solid, part i: low frequency rangeJournal of Acoustic Society, American 1956;28:168–77.
[18] Ou J. Three-dimensional numerical modelling of interaction between soil and pore fluid. PhD thesis, University of Birmingham, Birmingham, UK; 2009.
[19] Elgamal A, Parra E, Yang Z, Adalier K. Numerical analysis of embankment foundation liquefaction countermeasures. Journal of Earthquake Engineering 2002;6(4):447–71.
[20] Esrig MI, Kirby RC. Implication of gas content for predicting the stability of submarine slopes. Marine Geotechnology 1977;17:58–67.
[21] Pietruszczak S, Pande GN. Constitutive relations for partially saturated soils containing gas inclusions. Journal of Geotechnical Engineering, ASCE 1996;122(1):50–9.
[22] Mory M, Michallet H, Piedra-Cureva DBI, Barnoud JM, Foray P, Abadie S, et al. Constitutive relations for partially saturated soils containing gas inclusions. Journal of Waterway, Port, Coastal and Ocean Engineering, ASCE 2007; 133(1):28–38.